Efficiency of a reduced model of seismic metamaterials

Michaël Darche, Fernando Lopez-caballero, D. Aubry, B. Tie, B. Caicedo, F.J. Monroy Mendoza

Efficiency of a reduced model of seismic metamaterials

M. Darche, F. Lopez-Caballero, D. Aubry & B. Tie
Laboratoire MSSMat. CentraleSupélec, Université Paris-Saclay, France

B. Caicedo Hormaza & F. J. Monroy Mendoza
Civil and Environmental Department, Universidad de los Andes, Bogota, Colombia

ABSTRACT: In the present work, we deal with both analytical/numerical and experimental modelings of seismic metamaterials, designed to protect buildings and civil infrastructures from incoming seismic waves. By using Floquet-Bloch transform, it is possible to strongly reduce the size of numerical model compared to a fully simulated model. Indeed, the numerical modeling comes down to the study of the eigenproblems defined on a primitive cell representative of the whole periodic medium. Existence of frequency bandgaps, one of the main issues of metamaterial, is analysed. Moreover, using reduced laboratory samples of soil with periodically distributed holes or concrete inclusions, actual efficiency of the studied seismic metamaterials is tested and compared with the analytical/numerical prediction. The comparison highlights the similarities observed between experimentally recorded transfer functions and numerically predicted bandgaps.

1 INTRODUCTION

The response of a building facing a seismic signal depends on its own geometric and material properties, but also on both the incident waves and the characteristics of soil in the surrounding area. As the standardization of old structures to the current seismic risk cartography could be tricky, a modification of the soil around the buildings could be a promising alternative to improve their response by rerouting harmful waves.

On the one hand, several studies tended to analyze the effect of barriers or other architectured structures places in the ground to limit the propagation of the waves induced by ground vibrations (Avilès & Sánchez-Sesma 1983) or railway (Van Hoorickx et al. 2017). Both are based on the previous work of Lysmer & Waas (1972). Clouteau & Aubry (2001) analyzed how a dense urban area can influence the propagation of seismic waves, especially in the case of periodically placed buildings.

On the other hand, the academic work of Veselago (1968) about electromagnetism, considering materials with both negative permeability and negative permittivity, have enlightened a new branch of the fundamental physic research about architectured materials. Materials architectured with specific periodic (or non-periodic) sub-wavelength microstructures, called metamaterials, were designed for their unconventional properties. Research advances have been achieved first by the electromagnetic community with for example the use of negative refraction index metamaterials (Pendry et al. 1999, Pendry 2000).

The study and development of metamaterials in the seismic domain to protect structures from incoming waves, especially the surface waves, are more recent. For example, Kim & Das (2012), Ungureanu et al. (2016) used metamaterials to control seismic waves. Material and geometrical characteristics of the microstructure of a metamaterial play an essential role on its behaviour with respect to the wave propagation, parametric analyses are therefore necessary and several studies have been performed (e.g. Du et al. (2017)).

Beside the theoretical and numerical investigations, several *in-situ* experiments have been designed to show the feasibility of seismic protections with, for example, periodically distributed inclusions (Brûlé et al. 2014) or even natural metamaterials like forests (Colombi et al. 2016),

and to test their efficiency. Contrary to *in-situ* test, the experimentation on reduced models allows a better control of the different material parameters. For example, Colombi et al.'s study (2016) on the propagation of surface waves through a forest was preceded by laboratory experiments on reduced scale (Rupin et al. 2014). In laboratory models (reduced scale), in order to have an adequate replication of the *in-situ* stress field (full scale), several works have also been performed using centrifuge modeling. For example, isolation effects of geofoam barriers on wave propagation within soil were investigated using a centrifuge device by Murillo et al. (2009).

In the present work, two types of seismic metamaterials with periodically distributed holes or inclusions are numerically and experimentally investigated. In particular, the existence of frequency bandgaps is analyzed. It is indeed one of the most important issues of using metamaterials to control seismic waves, as it means the non-propagation of waves within some segmented frequency ranges due to the interactions between waves and the periodic microstructure. Based on the previously developed theoretical/numerical studies of periodic media made of beams or plates (Tie et al. 2013, Tie et al. 2016), new numerical models are built and theoretical frequency bandgaps are computed using Floquet-Bloch theory. Besides, reduced laboratory models of soil are designed and made. Then, their efficiency is tested and their coherence with numerical dispersion curves showing bandgaps is considered.

2 BLOCH WAVE BASED MODELING OF A PERIODIC MEDIUM

In order to study analytically the existence of frequency bandgaps due to the presence of inclusions or heterogeneities in a periodic media (Fig. 1), the Floquet-Bloch theory is used in this work. Thus, the following elastic wave equation is considered in the frequency domain, with $\mathbf{u}(\mathbf{x})$ the displacement field, $\mathbf{C}(\mathbf{x})$ the elasticity tensor, $\rho(\mathbf{x})$ the mass density and ω the angular frequency:

$$\mathbf{div}_{\mathbf{x}}\left(\mathbf{C}(\mathbf{x}) : \varepsilon(\mathbf{u}(\mathbf{x}))\right) = -\rho(\mathbf{x})\omega^2\mathbf{u}(\mathbf{x}) \tag{1}$$

In Equation 1, $\varepsilon(\mathbf{u})$ is the infinitesimal strain tensor defined as:

$$\varepsilon(\mathbf{u}) = \frac{1}{2}\left(\boldsymbol{\nabla}_{\mathbf{x}}\mathbf{u} + (\boldsymbol{\nabla}_{\mathbf{x}}\mathbf{u})^T\right) \tag{2}$$

In the case of a periodic medium, we have $\mathbf{C}(\mathbf{x} + \boldsymbol{\gamma}_{\boldsymbol{n}}) = \mathbf{C}(\mathbf{x})$ and $\rho(\mathbf{x} + \boldsymbol{\gamma}_{\boldsymbol{n}}) = \rho(\mathbf{x})$, $\forall \boldsymbol{n} \in Z^{dim}$, with $\boldsymbol{\gamma}_{\boldsymbol{n}} = \sum_{i=1}^{dim} n_i\mathbf{L}_i$, dim the dimension of the physical space, and $\mathbf{L}_i$ the vectors of periodicity (Fig. 1). Thanks to the periodicity of the periodic medium, the Floquet-Bloch transform allows giving a response on the entire medium with the modal analysis of the only primitive cell (Floquet 1883, Bloch 1928).

In fact, by the Floquet-Bloch transform a non-periodic field like $\mathbf{u}(\mathbf{x})$ defined on a periodic medium can be decomposed into periodic fields $\mathbf{u}^B(\mathbf{x}, \mathbf{k})$, which are called Bloch wave modes and are calculated as follows:

$$\mathbf{u}^B(\mathbf{x}, \mathbf{k}) = \sum_{\boldsymbol{n} \in Z^{dim}} \mathbf{u}(\mathbf{x} + \boldsymbol{\gamma}_{\boldsymbol{n}}) e^{i\mathbf{k}\,\cdot\,(\mathbf{x}+\boldsymbol{\gamma}_{\boldsymbol{n}})} \tag{3}$$

where $\mathbf{k}$ is the Bloch wave vector belonging to the Brillouin zone (Brillouin 1946).

According to Equation 3, it is obvious that the principle of the Floquet-Bloch transform is to sum up, over the whole periodic medium, values of the signal taken at all the periodically corresponding points (Fig. 1). The obtained Bloch wave modes are therefore periodic and have the same periodicity than the periodic medium.

The Floquet-Bloch transform applied to the initial problem defined by Equation 1 gives rise to the following eigenvalue problems:

$$(\mathbf{div}_{\mathbf{x}} + i\mathbf{k}) \cdot \left(\mathbf{C} : (\varepsilon(\mathbf{u}^B) + i\mathbf{k} \otimes_s \mathbf{u}^B)\right) = -\rho\omega^2\mathbf{u}^B \tag{4}$$

Hence, to solve the wave propagation problem on the whole periodic medium, it is sufficient to study eigenvalues and eigenmodes on the primitive cell. Because the eigenproblem (Equation 4) is too complex to be solved analytically, there is a need to use numerical methods.

Otherwise, according to Brillouin (1946), the eigenanalysis of Bloch wave modes can be limited to the first Brillouin zone, which is in fact the elementary cell in the reciprocal space dual to the primitive cell in the physical space. However, the eigenanalysis is finally done within a smaller zone, called the irreducible Brillouin zone, which is defined by taking into account the

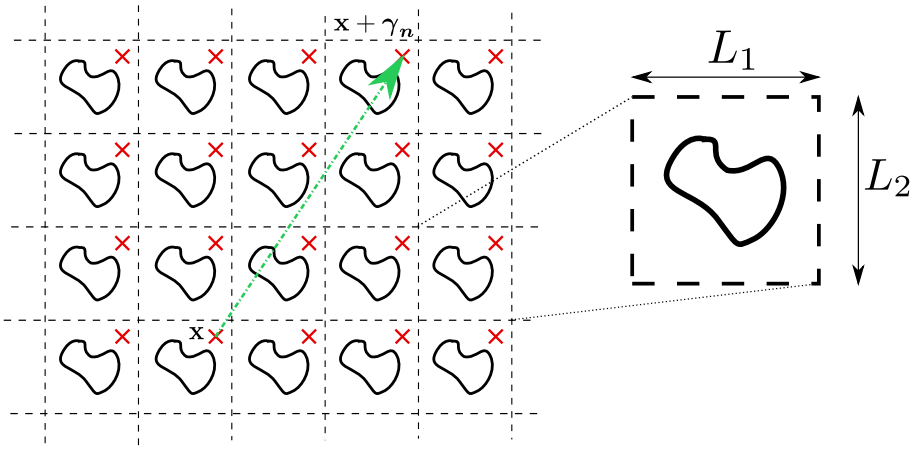

Figure 1. Example of periodic medium and its primitive cell

symmetries of the first Brillouin zone. In practice, a grid of discret points of k is used in the irreducible Brillouin zone, and for each Bloch wave vector k, the eigenproblem (Equation 4) is solved numerically using the finite element method.

To apply the finite element method to the eigenproblem (Equation 4), its weak form is developed as follows:

$$\int_\Omega \left(\mathbf{C} : (\boldsymbol{\varepsilon}(\mathbf{u}^B) + i\mathbf{k} \otimes_s \mathbf{u}^B)\right) : \overline{(\boldsymbol{\varepsilon}\,(\mathbf{v}^B) + i\mathbf{k} \otimes_s \mathbf{v}^B)} d\Omega = -\int_\Omega \rho\omega^2 \mathbf{u} \cdot \mathbf{v} d\Omega \tag{5}$$

with $\mathbf{v}$ virtual displacement field. To complete the definition of the above weak eigenproblem, appropriate periodic boundary conditions have to be applied on the primitive cell.

The primitive cell is discretized by a finite element mesh. In our study, a same finite element mesh is used whatever the value of $\mathbf{k}$.

3 REDUCED METAMATERIAL MODELS

In order to verify the efficiency of a non-infinite metamaterial compared to the prediction obtained by the Floquet-Bloch theory in an infinite periodic medium, an experimental study is made. The attenuation on the amplitude of some frequencies induced by the presence of inclusions is measured in the frequency domain. For that, a comparison of the obtained response at several points of an homogeneous block of compacted soil and the one with periodically distributed heterogeneities is done. In the experimental model, the heterogeneities are simulated using empty holes and concrete inclusions. It allows to assess the effect of the properties contrast between the inclusions and the soil matrix on both the occurence and the location of frequency bandgaps. In addition, the efficiency of each solution will be evaluated.

3.1 *Sample preparation and parameters*

As previously indicated, by using a reduced laboratory model, the properties of soil are easier to control than in an *in-situ* test. In the present work, the tested block is made of compacted kaolin soil. The consistency of the soil is chosen to have the water content adjusted around its optimum Proctor ($w_{opt} = 26\%$) to reduce the damping. The Proctor optimum water content corresponds to the highest mass density that can be achieved. Otherwise, to assure the assumption of homogeneity of the metamaterial's matrix adopted in the present work, the hydrated kaolin is passed through a sieve of $4\mathrm{mm}$ before the compaction.

To obtain a sample of size $300 \times 300 \times 250\mathrm{mm}^3$ (Fig. 2), the hydrated kaolin is compacted with three successive layers in its depth until a load of $1.1\mathrm{MPa}$ using a hydraulic press. The obtained compact kaolin soil has its density ρ_s equal to $1750\mathrm{kg/m}^3$, and its elastic modulus E_s is measured to be $233\mathrm{MPa}$, by calculating correlation between time signals recorded at different points (see Section 4) and with a Poisson ratio ν_s taken equal to 0.25.

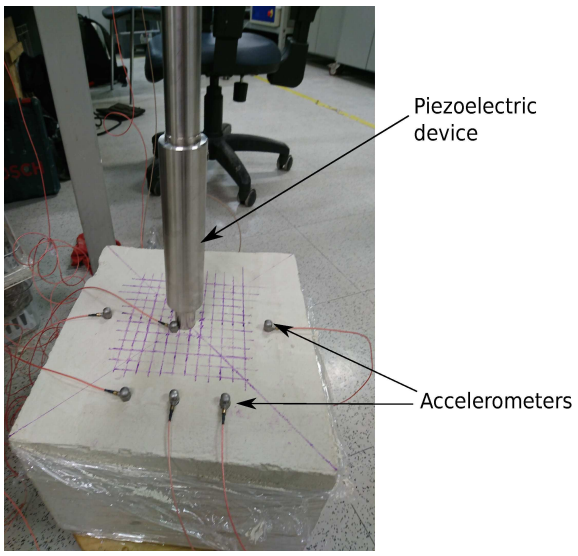

Figure 2. Presentation of the experimental setting: A homogeneous sample with the electronic devices

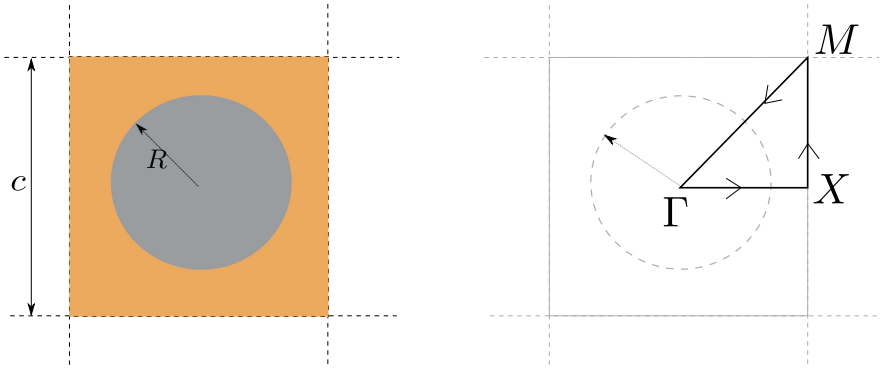

Figure 3. Primitive cell (left) and its Brillouin zone (right)

From homogeneous samples, metamaterial ones are made in such a way that they are periodic in the horizontal plane on a depth of $8\mathrm{cm}$ by drilling empty holes or by introducing inclusions. For the periodic layer, the primitive cell is designed as a 2D square pattern of dimension $c \times c = 13 \times 13\mathrm{mm}^2$ with cylindrical empty holes or inclusions with a radius R equal to $4\mathrm{mm}$ (Fig. 3).

Two types of metamaterial samples are made, with respectively empty holes or concrete inclusions as periodic heterogeneities. In the first case, holes are drilled using a broach with a diameter of $8\mathrm{mm}$. Because the holes are hand-made, there is a large uncertainty in their actual diameters and positions. For the second case, the holes drilled in the first case are filled by quick-setting cement, then tests are performed six days after pouring the concrete. Contrary to originally rigid inclusions such as metallic ones, cast-in-place concrete inclusions have the advantage of fitting the shape of the holes without the use of force, hence, a "prefect" adhesion on matrix/inclusion interfaces can be obtained without local modification of the properties of the compact kaolin soil. After compression tests on samples of concrete poured in the same way, the properties of the concrete inclusions are identified as: $E_c = 10\mathrm{GPa}$, $\rho_c = 2100\mathrm{kg/m}^3$ and $\nu_c = 0.3$.

3.2 *Boundary condition setting and experimental devices*

In order to reduce the influence of reflected waves, the sample is laid on a rubber layer. All its other boundaries are free surfaces.

The incident wave signal is generated with a piezoelectric device at the top horizontal boundary of tested samples (Fig. 2). Especially in our case surface waves are generated, as under an electrical signal, a piezoelectric crystal convert the energy into a stress field and it is therefore possible to control the type of introduced mechanical waves. For the sake of simplicity of experimental

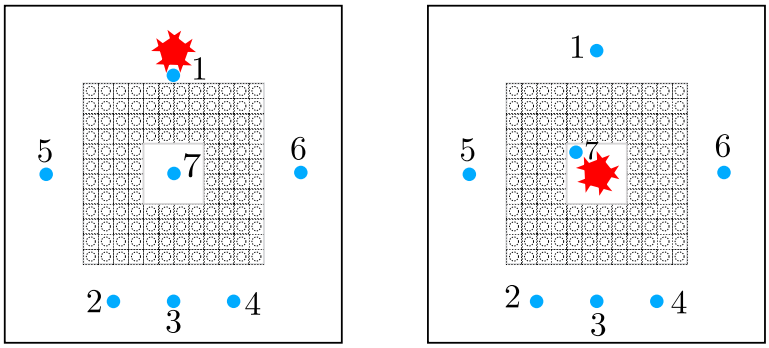

Figure 4. Top view of two different configurations for the positions of accelerometers (blue circles) and of the piezoelectric device (red)

setting, only monochromatic signals limited by 25kHz are produced by the piezoelectric device and applied on the tested samples. About twenty frequencies are considered. The lowest one is 200Hz.

For each frequency, the propagation of the signal is measured on the top horizontal surface by means of seven accelerometers (Fig. 2, Fig. 4). The accelerometers have an operational range until 20kHz. The sampling frequency is 100kHz on samples of 2s. As a first analysis of experimental results, only the signals recorded by the accelerometers 1, 3 and 7 (Fig. 4) are considered in this work.

3.3 *Experimental configurations*

Regarding the position of the piezoelectric device, two experimental configurations are tested: one with the source out of the metamaterial barrier and an other one with the source inside (Fig. 4). With the first configuration, it is expected to test the influence of metamaterial barrier on the propagation of the incoming wave, while with the second one, it is expected to investigate the behaviour of the waves trapped by the barrier within it. The same block of compacted soil is used for homogeneous sample and for the improved one. The homogeneous model will be used as a reference case. As the attenuation within metamaterial samples is measured with respect to the reference one, uncertainties on material properties and the lack of knowledge on boundary conditions could be considered as suppressed.

4 NUMERICAL/EXPERIMENTAL COMPARISON

2D numerical models based on the Floquet-Bloch theory presented here above (Section 2) are used to perform numerical/experimental comparison. They represent in fact plane wave propagation in an infinite 2D periodic domain with a primitive cell defined in Figure 3. It is worth noticing that, for the tested samples, neither the vertical direction, in which materials are homogeneous, nor its boundaries are not taken into account by the numerical model. Caution is therefore required in interpreting the comparison presented hereafter.

To set appropriate material properties in the numerical models, especially those of the compact soil, the classical method of cross-correlation (Elgamal et al. 2004) is used to estimate the Rayleigh wave velocity propagating in it. Cross-correlation function $c_{a_i a_j}$ between two temporal signals recorded by accelerometers $a_i(t)$ and $a_j(t)$ is expressed as:

$$c_{a_i a_j}(\tau) = \frac{\frac{1}{N-m}\sum_{n=1}^{N-m} a_i(n\Delta t)a_j((n+m)\Delta t)}{\sqrt{\frac{1}{N}\sum_{n=1}^{N} a_i^2(n\Delta t)}\sqrt{\frac{1}{N}\sum_{n=1}^{N} a_j^2(n\Delta t)}} \qquad m = 0, 1, 2, \ldots, N \tag{6}$$

with τ the time delay, N the length of the signal and Δt the time step of the signal.

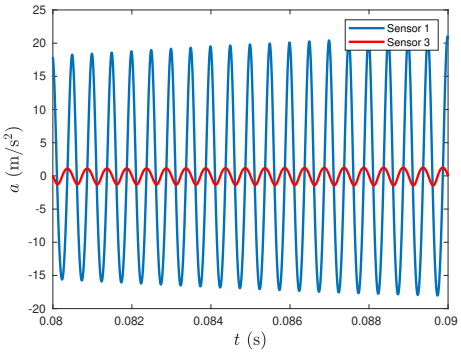

Figure 5. Temporal signals recorded at accelerometers 1 and 3 in the homogeneous sample tested within the first configuration (see Fig. 4 (left)). The frequency of the signal of 2s is 2MHz; A zoom of the temporal signal between 0.08s and 0.09s is presented.

For example, the cross-correlation between signals recorded at point 1 and 3 for the frequency equal to 4.25kHz results in a velocity of the Rayleigh waves of $V_R = 206$m/s. Then the Young's modulus of the compacted soil is determined using the following equation:

$$E_s = 2\rho_s(1+\nu_s)\cdot V_S^2 \tag{7}$$

with V_S the shear wave velocity linked to V_R by:

$$V_R = \frac{0.862 + 1.14\nu_s}{1+\nu_s} V_S \tag{8}$$

With the numerical models, eigenvalues for each discret $\boldsymbol{k}$ chosen in the irreducible Brillouin zone are computed by performing a finite element analysis of the primitive cell. Dispersion curves are then plotted and existence of frequency bandgaps can be highlighted.

For the data post-processing of experimental results, the transfer functions $\alpha(f)$ with respect to the frequency f is defined as the ratio of the signal recorded after the metamaterial barriers to the incident one:

$$\alpha_M(f) = \frac{\widehat{a}_7(f)}{\widehat{a}_1(f)}; \qquad \alpha_C(f) = \frac{\widehat{a}_1(f)}{\widehat{a}_7(f)} \tag{9}$$

with $\widehat{a}_i(f)$ the Fourier transform of the vertical accelerations measured with the sensor i. In Equation 9, α_M gives an estimate of attenuation for the first experimental configuration (see Figure 4(left)) and α_C for the second one (see Figure 4(right)). Finally, by calculating the ratio of $\alpha(f)$ obtained within a metamaterial sample to the one obtained within the homogeneous simple, the attenuation due to the metamaterial barriers can be actually measured without the one caused by the geometrical spreading of wavefront (visible on Fig. 5).

The Figure 6 presents the comparison between numerical predictions and experimental measures for both experimental configurations and for both cases of periodically distributed holes (top line in Fig. 6) or concrete inclusions (bottom line in Fig. 6).

- Figure (a) presents dispersion curves predicted theoretically by solving the eigenproblem (Equation 4) and computed using finite elements. The first Floquet-Bloch modes are shown within the frequency range $[0, 20]$kHz. In the case of the primitive cell with a hole, the first bandgap is obtained between 9.4kHz and 10.2kHz. In the case of the primitive cell with a concrete inclusion, the first frequency bandgap is obtained between 16.5kHz and 18.6kHz and is much larger.
- Figures (b)-(c) present the attenuation levels obtained experimentally in terms of the ratios between transfer functions. We note that, as the valid operating range of the accelerometers are inferior to 20kHz, experimental results at this frequency are questionable. For the metamaterial sample with holes, the experimental results appear coherent with the numerical predictions, as an important attenuation level is observed around 8kHz, close to the frequency range of the first numerically predicted bandgaps. For the metamaterial sample with concrete inclusions, the numerical/experimental comparison is less obvious. However, for the first experimental

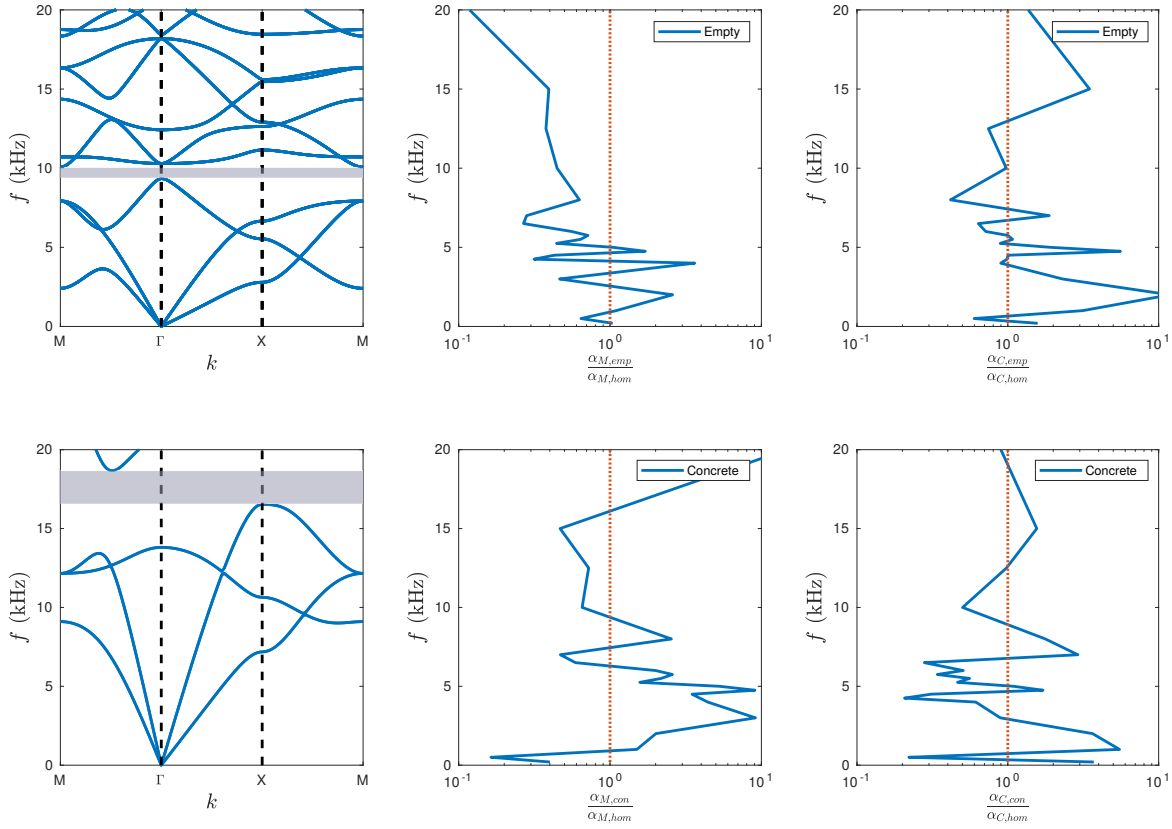

Figure 6. Comparison between the theoretically predicted frequency bandgaps (grey) and experimental transfer functions in the two cases of empty holes (first line) and concrete inclusions (second line). (a) Dispersion curves showing the first Floquet-Bloch modes and the first bandgap in the frequency range $[0, 20]$kHz. (b)-(c) Transfer functions for the two different configurations (Fig. 4).

configuration, a large frequency range of attenuation is observed between 10kHz and 15kHz, which is in agreement with the numerical predictions.

The comparison between numerical and experimental results is encouraging but not conclusive. Several possible causes can explain differences. First of all, the 2D numerical model is not representative of the 3D experiment, because the third vertical direction is ignored and the boundary conditions are not taken into account in the Floquet-Bloch theory. Moreover, there are uncertainties in the identified material properties, such as the value of Rayleigh wave velocity.

5 CONCLUSIONS

In this work, 2D numerical models based on Floquet-Bloch theory have been developed to study a periodic metamaterial by eigenanalysis of a primitive cell. It was used to locate frequency bandgaps by plotting dispersion curves.

In order to test actual efficiency of metamaterial, an experimental test has been made on a block of compacted soil with periodically distributed empty holes or concrete inclusions. Experimental results showed the existence of frequency ranges of attenuation. However, they did not fit well with the numerically predicted frequency bandgaps, which brought out the limits of the developed numerical model.

REFERENCES

Avilès, J. & Sánchez-Sesma, F. J. 1983. Piles as Barriers for Elastic Waves. *Journal of Geotechnical Engineering 109*(9), 1133–1146.

Bloch, F. 1928. Quantum mechanics of electrons in crystal lattices. *Z. Phys 52*, 555–600.

Brillouin, L. 1946. *Wave Propagation in Periodic Structures*. S.l.: McGraw Hill. OCLC: 498587574.

Brûlé, S., Javelaud, E., Enoch, S., & Guenneau, S. 2014. Experiments on Seismic Metamaterials: Molding Surface Waves. *Physical Review Letters 112*(13), 133901.

Clouteau, D. & Aubry, D. 2001. Modifications of the ground motion in dense urban areas. *Journal of Computational Acoustics 09*(04), 1659–1675.

Colombi, A., Roux, P., Guenneau, S., Gueguen, P., & Craster, R. V. 2016. Forests as a natural seismic metamaterial: Rayleigh wave bandgaps induced by local resonances. *Scientific Reports 6*, 19238.

Du, Q., Zeng, Y., Huang, G., & Yang, H. 2017. Elastic metamaterial-based seismic shield for both Lamb and surface waves. *AIP Advances 7*(7), 075015.

Elgamal, A., Yang, Z., & Stepp, J. C. 2004. Seismic downhole arrays and applications in practice. In *Proceedings of the International Workshop for Site Selection, Installation and Operation of Geotechnical Strong-Motion Arrays. Consortium of Organizations for Strong-Motion Observation Systems (COSMOS)*.

Floquet, G. 1883. Sur les équations différentielles linéaires à coefficients périodiques. *Annales scientifiques de l'École Normale Supérieure 12*, 47–88.

Kim, S.-H. & Das, M. P. 2012. Seismic waveguide of metamaterials. *Modern Physics Letters B 26*(17), 1250105.

Lysmer, J. & Waas, G. 1972. Shear waves in plane infinite structures. *Journal of Engineering Mechanics*.

Murillo, C., Thorel, L., & Caicedo, B. 2009. Ground vibration isolation with geofoam barriers: Centrifuge modeling. *Geotextiles and Geomembranes 27*(6), 423–434.

Pendry, J. B. 2000. Negative Refraction Makes a Perfect Lens. *Physical Review Letters 85*(18), 3966–3969.

Pendry, J. B., Holden, A. J., Robbins, D. J., & Stewart, W. J. 1999. Magnetism from conductors and enhanced nonlinear phenomena. *IEEE Transactions on Microwave Theory and Techniques 47*(11), 2075–2084.

Rupin, M., Lemoult, F., Lerosey, G., & Roux, P. 2014. Experimental Demonstration of Ordered and Disordered Multiresonant Metamaterials for Lamb Waves. *Physical Review Letters 112*(23), 234301.

Tie, B., Tian, B. Y., & Aubry, D. 2013. Theoretical and numerical investigation of HF elastic wave propagation in two-dimensional periodic beam lattices. *Acta Mechanica Sinica 29*(6), 783–798.

Tie, B., Tian, B. Y., & Aubry, D. 2016. Theoretical and numerical modeling of membrane and bending elastic wave propagation in honeycomb thin layers and sandwiches. *Journal of Sound and Vibration 382*, 100–121.

Ungureanu, B., Achaoui, Y., Enoch, S., Brûlé, S., & Guenneau, S. 2016. Auxetic-like metamaterials as novel earthquake protections.

Van Hoorickx, C., Schevenels, M., & Lombaert, G. 2017. Double wall barriers for the reduction of ground vibration transmission. *Soil Dynamics and Earthquake Engineering 97*, 1–13.

Veselago, V. G. 1968. The electrodynamics of substances with simultaneously negative values of ε and μ. *Soviet Physics Uspekhi 10*(4), 509.